JOINT EUROPEAN TORUS

JET–P(92)78

R. Lasser, B. Grieveson, J.L. Hemmerich, R. Stagg, T. Dowhyluk,
K. Torr, R. Massey, P. Chambers and JET Team

Gas Chromatographic Analysis of the Gas Compositions in the Active Gas Handling Plant of JET

Gas Chromatographic Analysis of the Gas Compositions in the Active Gas Handling Plant of JET

R. Lasser, B. Grieveson, J.L. Hemmerich, R. Stagg, T. Dowhyluk[1], K. Torr[1], R. Massey[2], P. Chambers[3] and JET Team*

JET-Joint Undertaking, Culham Science Centre, OX14 3DB, Abingdon, UK

[1]EG & G Labserco Ltd, Oakville, Ontario, Canada.
[2]Ontario Hydro Research Division, Toronto, Ontario, Canada.
[3]Canadian Fusion Fuels Technology Project, Mississauga, Ontario, Canada
** See Annex*

Preprint of Paper to be submitted for publication in
Review of Scientific Instruments

ABSTRACT.

A gas chromatographic system for the analysis of gas species to be collected from the JET Torus and to be processed in the JET Active Gas Handling plant during the Active Operation Phase with deuterium and tritium plasmas was designed and built by CFFTP under contract with JET. A detailed description of the specifications of the system, of the system itself and of its performance will be given which was evaluated using several calibrated gas mixtures including test runs with tritiated species at JET.

Introduction

The Active Gas Handling (AGH) plant /1/ built for the tritium phase at JET consists of interlinked subsystems to receive, purify, store and recycle the gases from the Torus. One of these subsystems is the Analytical Laboratory (AN) /2/ which is connected via sampling lines to the other systems. Three analytical techniques using a) an omegatron and a quadrupole mass spectrometer, b) a gas chromatograph and c) ionisation chambers will be used in AN for the characterisation of the different gas mixtures of the AGH plant.

Hydrogen isotopes will be the 'burning fuel' for future fusion reactors. At JET mainly pure H_2, D_2 and/or T_2 are or will be injected into the Torus. After a plasma shot the exhaust gas consists of the six hydrogen molecules H_2, HD, HT, D_2, DT and T_2 (mainly unburnt fuel, partly recycled from the first wall), helium ('ash'), methane and higher hydrocarbons, etc. (impurities). In case of leaks and/or 'dirty' inner walls also other impurities such as nitrogen, oxygen, argon, water, carbon dioxide, carbon monoxide, etc. will be present. These impurities are normally in the low percentage range. The exhaust gas mixture of the Torus will be collected and separated in the AGH plant resulting in very wide concentration ranges of the different gas species which must be characterised.

Whereas the gas chromatographic separation and detection of the six hydrogen molecules is well documented /3-8/, the information on gas chromatographic systems, which address the task of analysing all gas species expected from an experimental fusion machine in a single analysis run, is very limited/9/.

This paper will present the JET analytical gas chromatographic (GC) system focusing on its objectives, design and performance.

Requirements for the JET analytical GC-system

The JET analytical GC-system should fulfil the following requirements:

a) The analytical GC-system shall separate and detect all mixtures of the six hydrogen molecules Q_2 (Q standing for protium, deuterium and tritium) and helium within the concentration range of 100 ppm to 100 %. Helium-3 and helium-4 need not be separated. In addition, concentrations of carbon monoxide and carbon dioxide between 100 ppm and 50 %, of methane, higher hydrocarbons and nitrogen between 10 ppm and 98 % , of oxygen between 10 ppm and 22 % and of water between 10 ppm and 4% must be detected. In this way all gas species expected to be present in the torus exhaust gas or to be handled in the AGH-plant can be detected within the concentration ranges of interest.

b) The time to analyse any gas mixture consisting of the gas species mentioned under point a) shall be shorter than one hour. This specification influences the choice of column for the separation via the retention time and offers the possibility for several GC-runs per working day.

c) Tritium sensitive detectors, e.g. ionisation chambers (IC's), flow proportional counter detectors (FPCD's), etc, shall be used in addition to the detectors usually used in gas chromatography such as thermal conductivity detectors (TCD's), flame ionisation detectors (FID's), helium ionisation detectors (HeID's), etc. This allows the independent analysis of tritiated gas species such as tritiated hydrogen, tritiated methane, tritiated water and tritiated higher hydrocarbons.

d) A compression stage shall pressurise gas mixtures of low pressure to the injection head pressure of the GC-system. This allows the injection of equal gas

amounts into the GC-system ensuring equal lower detection limits and easy comparison of area counts or concentrations between independent GC-runs.

e) Up stream pressure regulators shall be used in the exhaust lines of the GC-system to allow transfer of the exhaust gases to other systems (e.g. tritium removal systems) via pumps prior to their release into the atmosphere. The up stream pressure regulators avoid evacuation of the GC-system and allow adjustments of the GC-exit pressure in relation to the pressure of ambient atmosphere.

f) The equipment to be used for the process shall be tritium compatible. This specification ensures that equipment and materials which are known to deteriorate in the presence of high tritium concentrations such as rubber-O-rings, etc, are not used.

g) The He leak rate of the containment for the process shall be as small as possible to minimise tritium releases into the environment and its contamination.

h) The space needed by the process equipment shall be smaller than 60*55*55 cm^3, because due to stringent safety considerations the GC-equipment will finally be placed into a glove box, where the connection to the manifolds with the sampling lines to the different subsystems of the AGH-plant will be made.

i) Process management of the GC-system must be organised such that routine analysis can be performed without the need to manually operate equipment of the GC-system inside the glove box.

Description of the JET analytical GC-system

A) General remarks:

Gas chromatographic separation of the 6 hydrogen molecules can be achieved by columns cooled down to liquid nitrogen temperatures/3-7/. At these temperatures most of the impurities (hydrocarbons, O_2, N_2, CO, CO_2, water, etc.) would be trapped in the columns before reaching a detector.

Normally a two stage process is used for the analysis of hydrogen isotopes and impurities where the impurities are analysed either before or parallel to the Q_2 molecules. Detecting the impurities in a first step offers the chance that the fast eluting species (helium and hydrogen) can be so far separated from the impurities that only helium and hydrogen will be injected into the low temperature column via switching of special valves. This method avoids deterioration of the column performance for hydrogen separation and finally clogging of the columns due to trapping of impurities.

B) Mechanical description:

Fig. 1 shows schematically the flow diagram of the JET GC-system. The manifold to supply the gases for injection and the pump for transfer of the exhaust gas are not presented.

The GC-system can be separated into three parts, a) a compression stage, b) system 1 for detection of helium, the six hydrogen molecules, oxygen, nitrogen, methane via a TCD and of HT, DT and T_2 via a FPCD and c) system 2 for detection of

hydrocarbons, carbon monoxide, carbon dioxide via a FID and of tritiated hydrogen and hydrocarbons via a FPCD.

The detectors, Valco valves and most of the process lines are mounted inside a secondary containment.

In the following part the equipment will be discussed in more detail.

a) Compression stage:

The pressure of the gas mixtures of the AGH-plant will vary over a wide range. Therefore, a compression loop was built for the injection of equal gas amounts into the GC-system to allow easy analysis and comparison of measured area counts. Furthermore, no pressure fluctuations are created inside the GC-system during injection if the compression pressure of the loop equals the column head pressures next to the inlets of the first columns of both systems.

Gases with pressures between 30 kPa and 330 kPa can be compressed inside a capillary to the injection pressure using carrier gas.

The compression is performed in the following way: after evacuation of the capillary the gas to be analysed can enter the compression loop via valve VA-7261 and will be compressed by opening the valve VA-7510. The down stream pressure regulator PRD-7521 guarantees the same compression pressure. The temperature of the capillary is kept at 323 K. These conditions of constant temperature, of equal volume and pressure allow the injection of reproducible gas amounts of 0.015 Pam^3 into the systems 1 and 2 via switching the Valco valve VX-7512 .

b) System 1:

The main parts of system 1 are: 2 additional Valco-valves (VX-7513 and VX-7514), 2 off 1/8"*6' stainless steel columns (COL-7541 and COL-7542) packed with molecular sieve 13X 45/60 mesh, a 1/8"*4' stainless steel column (COL-7543)

packed with HayeSepD 60/80 mesh, a 1/8"*1.5 m copper column (COL-7544) packed with alumina doped with iron 100/120 mesh, a TCD and FPCD. The first three columns are kept at 323K inside an auxiliary oven whereas the copper column is kept at 77K in a liquid nitrogen dewar.

The molecular sieve columns are used for separation of He, Q_2, O_2, N_2, CH_4, CO and the HayeSepD column mainly for analysis of water. Valco valve VX-7513 is used to bypass the molecular sieve columns because otherwise the water would be absorbed. Valco valve VX-7514 can be switched such that only He and Q_2 are injected into the copper column for further separation. The iron doping of the alumina promotes the ortho-para interconversion which would otherwise result into separate peaks for ortho- and para-hydrogen.

Gas species eluting form the first three columns and from the copper column are measured by the same TCD. This means that the column length should be chosen in such a way that gas species eluting from the columns enter the TCD with sufficient time differences to avoid overlap.

A splitter built by capillaries of different lengths assures that only about one percent of the carrier gas flow reaches the FPCD. This extends the upper operational range of the very sensitive FPCD.

c) System 2:

The main parts of system 2 are: a 1/8"*12' stainless steel column (COL-7540) packed with HayeSepQ 60/80 mesh, a methaniser, a FID and a FPCD.

The purpose of system 2 is to separate and detect CO, CH_4, CO_2, higher hydrocarbons and tritiated hydrogen and hydrocarbons. The separation is done via the HayeSepQ column which is temperature cycled in the GC-oven to reduce the retention times of the higher hydrocarbons.

The neon carrier gas leaving the HayeSepQ column is divided into two streams: one is injected into the methaniser and FID and the other into the FPCD. Again a splitter is used in front of the FPCD.

CO and CO_2 are converted to methane by a commercially available methaniser.

d) Multiple containment:

In most GC-systems the leak tightness is only of importance insofar as the analysis should not be affected by the gas surrounding the equipment. Most GC-systems vent into the atmosphere. The gas pressure inside the process lines is larger than outside and leakage occurs mainly to the outside. Thus many parts of a GC-system such as special detectors, Valco valves, mass flow controllers, etc, do not fulfil the stringent leak rate requirements used for handling radioactive gases such as tritium.

The solution for achieving very small leak rates and still using commercially available equipment (maybe with modifications to improve the leak tightness) was to build a secondary containment around all parts prone to leak. The only process components placed outside the secondary containment are tubes and Nupro valves with leak rates smaller than 10E-10 Pam^3/sec.

The boundaries of the secondary containment are shown in Fig 1 . The He leak rate of the secondary containment determined via evacuation was found to be smaller than 5*10E-9 Pam^3/sec. Considering the fact that during normal operation the pressure inside the secondary containment will be only a few mbars below atmosphere the expected tritium leak rate is probably more than 100 times smaller.

The secondary containment is purged via a continuous N_2 flow and the pressure inside can be adjusted via an upstream pressure regulator.

One disadvantage to rely mainly on the very small leak rates of the secondary containment and accepting higher leak rates of the process lines is that the inside of

the secondary containment may become contaminated making maintenance or repair work difficult.

C) GC control system:

The GC-system can be controlled manually or automatically. The status of the actuated valves and Valco valves is shown on a mimic. Fault conditions, e.g. insufficient pressure of a supply gas (Ne, H_2, P-10, synthetic air) or failure of the valve position micro switches to respond will be indicated and allow no further injection.

A logic controller (PLC) evacuates, fills and pressurises the compression loop.

The GC data system comprises a VARIAN DS-654 intermediate chromatography data handling package which allows monitoring the operation of the GC-system, collecting data of up to four detectors and plotting data in real time.

D) More specific data of the GC-system:

a)Temperatures:

During normal operations the auxiliary oven which contains the compression loop, the Valco valves VX-7512 and VX-7513 and the molecular sieve and HayeSepD packed columns is kept at 323K. The oven will only be heated to 353 and 523 K for water analysis and conditioning of the columns, respectively. Valco valve VX-7514 is not heated. The alumina packed column is kept at 77K. The temperature of the TCD oven is kept at 343K and increased to 353K for analysis of water. The HayeSepQ filled column is usually kept at 323K, but will be heated after a holding time of 2 minutes with a rate of 10 degree per minute to the final temperature of 473 K during every measurement. The methaniser operates at 648K.

The temperature of most other components is near room temperature. The only exceptions are the FID, its exhaust tube and the process up stream pressure

regulator. The latter two are heated to about 363K to keep the gas mixture above its dew point temperature.

b) Flow rates:

The flow rates of the neon carrier gas for system 1 and 2 are 20 and 25 cm^3 per minute, respectively. Hydrogen is supplied to the methaniser and FID at a flow rate of 27 cm^3 per minute, synthetic air to the FID and P10 gas to the FPCD at a flow rate of 275 and 50 cm^3 per minute, respectively. Two stage pressure regulators and mass flow controllers keep these flows constant.

The splitters in front of the FPCD's reduce the Ne carrier gas flow reaching the FPCD to 0.2 cm^3 per minute.

When helium is used as carrier gas, the setting of the mass flow controllers will not be changed. The flow for helium is about a factor of 1.6 higher than for neon due to their different viscosities.

c) Gases:

The purity of the neon gas is better than 99.995 percent. In addition, the neon gas passes through a heated metal bed which getters water and oxygen. The synthetic air is a mixture of 20.5 vol% oxygen and 79.5 vol% nitrogen with purities better than 99.995 and 99.999 percent, respectively. The P10 gas is a 10 vol% methane (purity > 99.99 vol%) in 90 vol% argon (purity > 99.995 vol%).

If a higher sensitivity is needed for oxygen, nitrogen, methane and water, helium (purity > 99.999 vol%) can be used as the carrier gas.

d) Valves:

The valves used are Nupro valves (size 4, all metal with Vespel tip) and Valco valves (WT serie) with the body made of Nitronic-60 and the seals made of carbon and PTFE filled polyimide.These valves can be operated at temperatures up to 573K.

e) Tubing:

Mainly stainless steel tubes of 1/16, 1/8 and 1/4" diameter are used. The connections inside the secondary containments are made with Swage-lok fittings, outside with Cajon VCR-connectors.

f) TCD:

The TCD is a commercial detector. Three different ranges of sensitivity can be chosen: 5.00, 0.50 and 0.05.

g) FID:

Commercial FID's vent directly into atmosphere. This is not acceptable, since tritiated water would be released into the secondary containment. A 'sealed' chimney was built around the FID, but the final leak test showed that the FID was still the most leaking part of the process lines.

Five different ranges of sensitivity can be chosen for FID currents between 10E-12 and 10E-8 A.

h) FPCD's:

FPCD's were built with an active cell volume of 20 cm^3 and a very thin inner electrode. Fig. 2 shows the plateau of events as a function of applied voltage measured with a radioactive source Cs-137. The counter of the FPCD's can collect up

to 32768 events and the counting time can be varied between 0.08 and 100 seconds.

Performance of the GC-system

The GC-system was tested with calibrated gas mixtures, four of them are listed in table 1. The performance of the GC-system will be demonstrated by results obtained with these mixtures.

A) Linearity of the GC-system:

Figs. 3a and b show the area counts under the peaks of gas mixture 1 and 2 (see table 1), respectively, as a function of the pressure of the compression loop. The gas amount injected into the GC-system is strictly proportional to the pressure (measured by a highly accurate capacitance manometer) as temperature and volume of the injection loop are kept constant. The area counts as measured by the TCD and FID are shown on the left and right side of the figs. 3a and b, respectively. The TCD and FID ranges are also presented.

Linear response was observed for all gas mixtures. The only exception observed is carbon dioxide for concentrations in excess of 1%. This deviation from linearity is caused by the methaniser, when the carbon dioxide concentrations are too high for full conversion to methane. Carbon monoxide is expected to show a similar behaviour, although the start of deviation from linearity should occur at higher concentrations due to the lower stability of carbon monoxide in comparison to carbon dioxide.

The O_2 peak is the sum of the H_2, HD and D_2 peaks if one considers that the O_2 peak was measured with the TCD range equal 0.50.

The TCD sensitivities fo the gas species shown in figs. 3a and b decrease in the sequence H_2, HD, He, D_2, N_2 = O_2 and CH_4 if one considers their concentrations in the mixtures.

B) Drift test of the GC-system:

The stability of the GC-system was tested measuring gas mixtures 1 and 2 for 20 days under the same conditions using compressed samples for injection. No long term drift of the area counts of the peaks was observed exceeding the normal scatter.

C) Retention time as a function of column temperatures and column heating rates:

Fig. 4a presents the retention time of gas species passing through system 1 as a function of the temperature of the columns filled with molecular sieve and HayeSepD. The gas species pass faster through the columns with increasing temperature and their retention time decreases in the sequence CO, CH_4, N_2, O_2, O_2 and He. The separation between the gas species will be best at lower temperatures (for most of our work we selected 323 K for the column temperature of system 1) with the disadvantage that the CO peak will overlap with the H_2 peak eluting from the l N_2 cooled column (see fig. 7).

Fig 4b shows the retention time of gas species detected by the FID as a function of the heating rate of the HayeSepQ filled column in system 2. The gas species are pushed faster through the column with increasing heating rate and the retention time decreases in the sequence: C_3H_8, C_2H_6, C_2H_2, C_2H_4, CO_2, CH_4 and CO. Best separation is achieved with a low heating rate (selected value: 10 degree per minute). Only C_2H_4 and C_2H_2 overlap slightly.

D) Chromatograms obtained by the GC-system:

1) Chromatograms of gas mixture 1 (see table 1):

The TCD chromatograms of gas mixture 1 obtained with neon and helium as carrier gas are shown in Figs. 5a, 5b and 5c, respectively. The difference between the two lower TCD chromatograms is that in picture a) the liquid nitrogen cooled column was bypassed, whereas in Fig. 5b the sample was sent through all columns of system 1 resulting in the second helium peak measured on the reference side of the TCD. Bypassing the Alumina column is achieved via switching Valco valve VX-7514. To obtain a positive second helium peak it is necessary to reverse the signal polarity of the TCD, because the helium goes though the reference side of the TCD when observed the second time. The peak height of the second helium peak is smaller than the first one mainly because of the slight broadening effect with longer retention times, but the area counts of both peaks are equal. The polarity must not be changed again, because the three later eluting gas species have lower thermal conductivities than neon. Carbon dioxide is not seen in the TCD chromatograms, because it is absorbed in the columns filled with molecular sieve.

Fig. 5c is the same gas mixture chromatographed with helium carrier. Under these conditions only three peaks are observed in the TCD chromatogram, because helium cannot be detected. The same chromatograms are obtained independent of passing through or bypassing the Alumina column. The shorter retention times are mainly due to larger flow rates of helium through the mass flow controllers set for standard neon flow and the different efficiences of Ne and He as carrier gas.. The O_2, N_2 and CH_4 peaks are about eight times larger with helium carrier gas instead of neon as expected from the differences in thermal conductivities.

2) Chromatograms of gas mixture 2 (see table 1):

Fig. 6a shows the TCD chromatogram of gas mixture 2 obtained with neon carrier gas. The O_2 peak is presented with low attenuation to make the first and second helium peak visible. The second helium peak is in fact a negative peak sitting on the high retention time side of the O_2 peak. The polarity is reversed at 2.80 minutes to obtain positive peaks for the other gas species in mixture 2. The hydrogen molecules are well separated by the Alumina column.

Fig. 6b presents the same chromatogram with helium as the carrier gas. Again helium is not detected and the retention times are shorter as discussed above. The main difference is that the H_2 peak is now much smaller than the D_2 peak which is due to an anomaly in the thermal conductivity of H_2 gas in helium. The thermal conductivity of low concentrations of H_2 gas in helium is lower than the one of pure helium. This explains the positive H_2 peak in Fig. 6a. Due to this anomaly helium cannot be used as carrier gas for direct analysis of hydrogen gas mixtures using a TCD.

The hydrogen peaks of fig. 6b are more asymmetrical than the ones of fig. 6a. This is not caused by the different carrier gas, but by the fact that in fig. 6b a three times larger sample was injected than in fig. 6a. If the sample size exceeds the design capacity of the column, a certain part of the sample does not find enough 'trapping centers' and passes too fast through the columns contributing mainly to the low retention side of the peaks.

3) Chromatograms of gas mixture 3 (see table 1):

Fig. 7 shows two TCD chromatograms and one FID chromatogram of mixture 3. Carbon dioxide and the hydrocarbons with the exception of methane are not detected by the TCD because they are absorbed in the molecular sieve filled columns before

reaching the TCD. Neon is not detected because it is used as carrier gas. The O_2, N_2, CH_4, CO and first He peaks are measured by passing through the sample side of the TCD, whereas the second He, H_2 and D_2 peaks are observed by passing through the reference side. One can see that the H_2 and CO peaks overlap partially. This was already concluded from the plot of the retention times as a function of column temperature in fig. 4 and it shows that the lengths of the different columns were not perfectly matched. One way to avoid overlapping of the CO and H_2 peaks is to switch the Valco valve VX-7513 after the detection of methane to stop the CO peak from reaching the TCD. Fig. 7a shows such a result: a well isolated H_2 peak is seen, but in front of it a new very narrow peak appears which is caused by pressure changes due to the Valco valve switching.

Fig. 7c presents the FID chromatogram of the five hydro carbons, carbon monoxide and carbon dioxide of the gas mixture 3. All peaks are well separated. The width of the peaks increases with increasing retention times.

4) Chromatogram of the gas mixture 4 (see table 1):

The TCD chromatogram of fig. 8a shows all species of the gas mixture 4 with the exception of neon, because neon is used as carrier gas. All peaks are positive due to the polarity reversal just in front of the second helium peak. The chromatogram is obtained with a TCD filament temperature of 623 K and a filament current of 208 mA and the sample was compressed to 390 KPa. These higher settings (the usual values are: TCD filament temperature at 523 K with a filament current of 164 mA) were selected to enhance sensitivity. After about 11 minutes the six hydrogen molecules start to elute - well separated and detected.

Fig. 8b) presents the FID chromatogram in its most sensitive range. The three last peaks can be attributed to carbon monoxide, methane and carbon dioxide.These species were not added to the mixture, so they are considered to be impurities which may have been created during the half a year storage time of the gas mixture in a

stainless steel container before its use. No hydrocarbon is known to elute faster than methane, so the only explanation of the first peak is that the FID is capable to detect the ionisation caused by tritium decay. The retention time of the peak is in agreement with the retention time of hydrogen.

The FPCD chromatogram of system 1 is presented in fig. 8c. The three peaks correspond to HT, DT and T_2 and coincide with the peaks measured by the TCD. The FPCD is so sensitive that the high voltage had to be reduced to 2200 volts and the counting time to 0.17 seconds to avoid over loading of the counter.

Fig. 8d presents the FPCD chromatogram of system 2. The only detected peak is attributed to the sum of the tritiated hydrogen molecules ($HT+DT+T_2$) and shows the same retention time as the first peak of the FID chromatogram confirming its interpretation. The applied voltage was 2000 volts and the counting time 0.08 seconds.

Conclusion

The gas chromatographic system built for the JET Active Operation Phase with tritium meets the requirements on sensitivity, linearity, stability, separation and resolution. It is capable of detecting the different gas species He, Q_2, O_2, N_2, CO, H_2, HD, HT, D_2, DT, T_2, CO_2 , CH_4 , higher hydrocarbons and their tritiated compounds in the specified concentration ranges from ppm levels up to 100 percent. The required minimum detection limits for the TCD can be achieved with large injected sample amounts and high filament currents. Due to the high sensitivity of the flow proportional counter detectors ppb levels of tritiated gas species will be detected which will be very useful during the tritium commissioning phase.

References:

/1/ R. Haange, P. Ballantyne, A. C. Bell, S. J. Booth, C. J. Caldwell-Nichols, P. Chuilon, J. L. Hemmerich, J.-F. Jaeger, A. Konstantellos, R. Lässer, G. Newbert, D. Wong and M. E. P. Wykes: Fusion Technology 21, 253 (1992).

/2/ R.Lässer, C.J. Caldwell-Nichols, J. Dallimore, B. Grieveson,J. L. Hemmerich, A. Konstantellos, M. Laveyry, P. Milverton, R. Stagg and J. Yorkshades: Fusion Technology 21, 406 (1992).

/3/ W.R.Moore and H.R.Ward: J.Phys. Chem. 64, 832 (1960).

/4/ J.King: J.Phys,Chem. 67, 1397 (1963).

/5/ C.Genty and R.Schott: Analytical Chemistry 42, 7 (1970).

/6/ T. Schober and C. Dieker: Rev.Sci.Instrum. 58, 1116 (1987).

/7/ R. Vogd, H. Ringel, H. Hackfort, T. Schober and C. Dieker: Fusion Technology 14, 574 (1988).

/8/ C. H. Cheh: Fusion Engineering and Design 10, 309 (1989).

/9/ M. Tanase, K. Kurosawa, M. Fujie, H. Sugai, S. Okane and M. Kato: Fusion Technology 14, 1090 (1988).

Table 1:

Gas mixture 1: 71.0% He, 1.5% O_2, 3.0% N_2, 1.6% CH_4 and 22.9% CO_2.

Gas mixture 2: 0.2% He, 0.4% N_2, 0.4% CH_4, 24.6% H_2, 50.4 % HD and 24.0 D_2.

Gas mixture 3: 2.9% He, 5.0% N_2, 4.5% H_2, 4.7% D_2, 7.5% CO, 3.9% CH_4, 5.1% CO_2, 3.1% C_2H_4, 3.0% C_2H_6, 3.0% C_2H_2, 3.0% C_3H_8 and 54.3% Ne.

Gas mixture 4: 0.964% He, 1.409% H_2, 0.806% HD, 0.817 % HT, 0.131% D_2, 0.282 DT, 0.163% T_2, rest Ne and very low level of impurities: CO, CH_4 and CO_2.

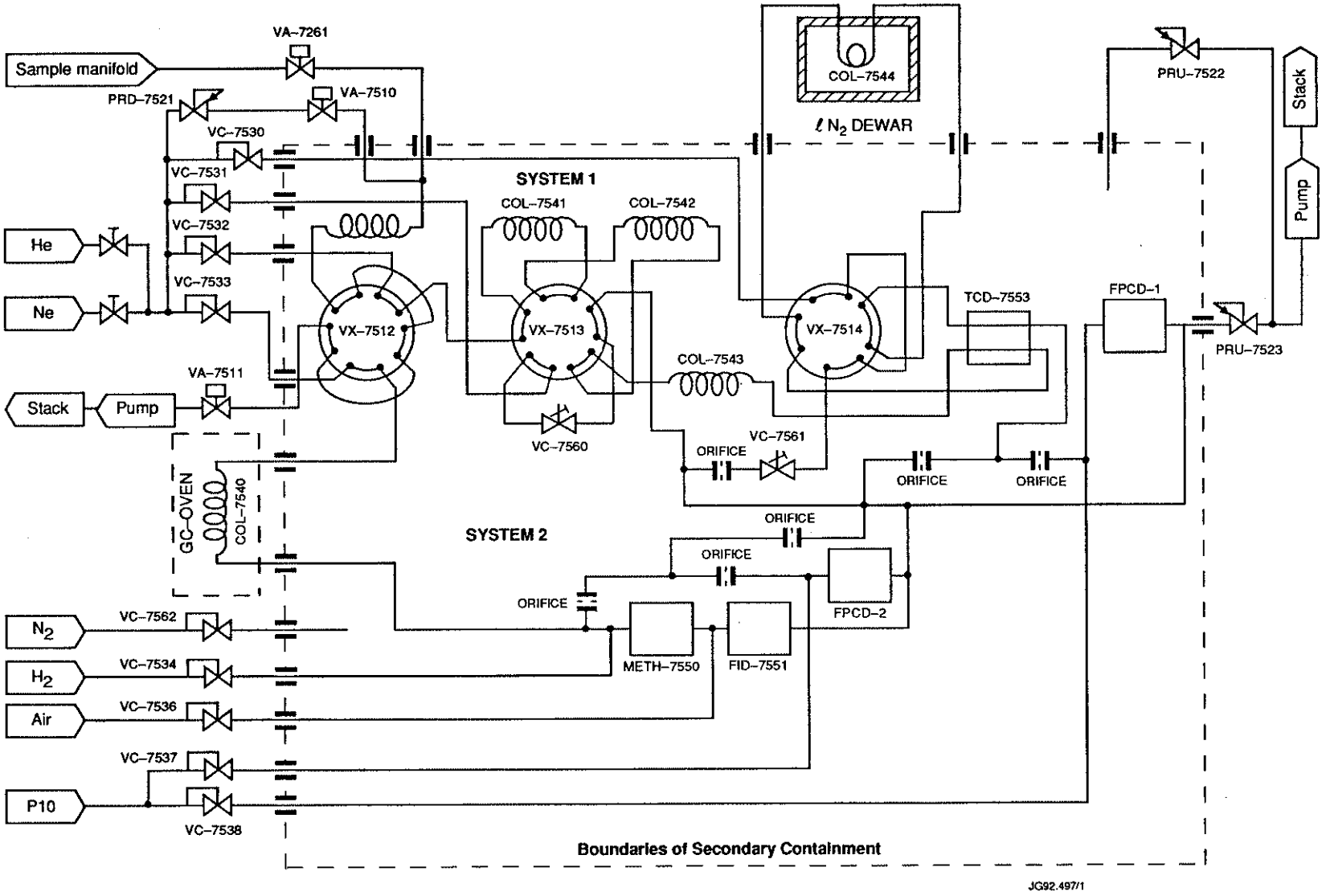

Fig.1: Schematic flow diagram of the GC-system: COL stands for column, VA for actuated valve, VM for manual needle valve, VC for mass flow controller, VX for Valco valve, PRD for down stream pressure regulator, PRU for up stream pressure regulator, TCD for thermal conductivity detector, FPCD for flow proportional counter detector, METH for methaniser and FID for flame ionisation detector.

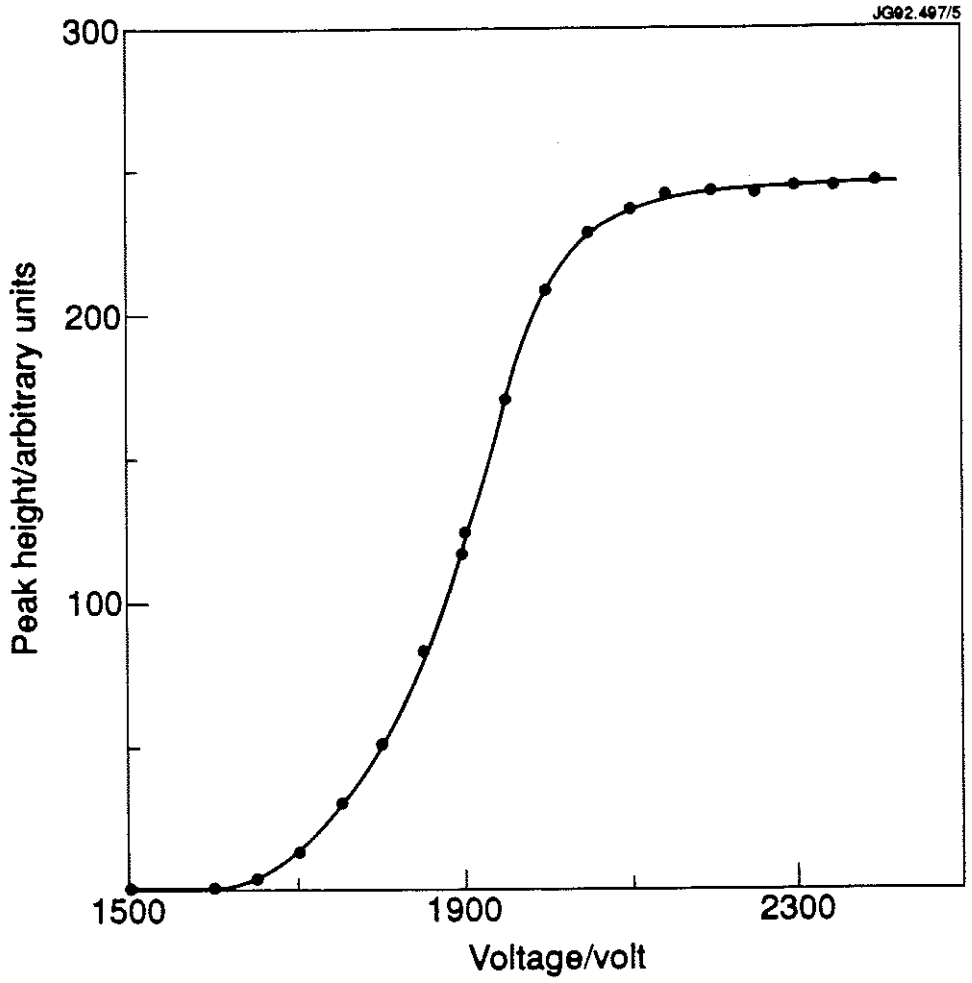

Fig. 2: Plateau characteristic of a flow proportional counter detector.

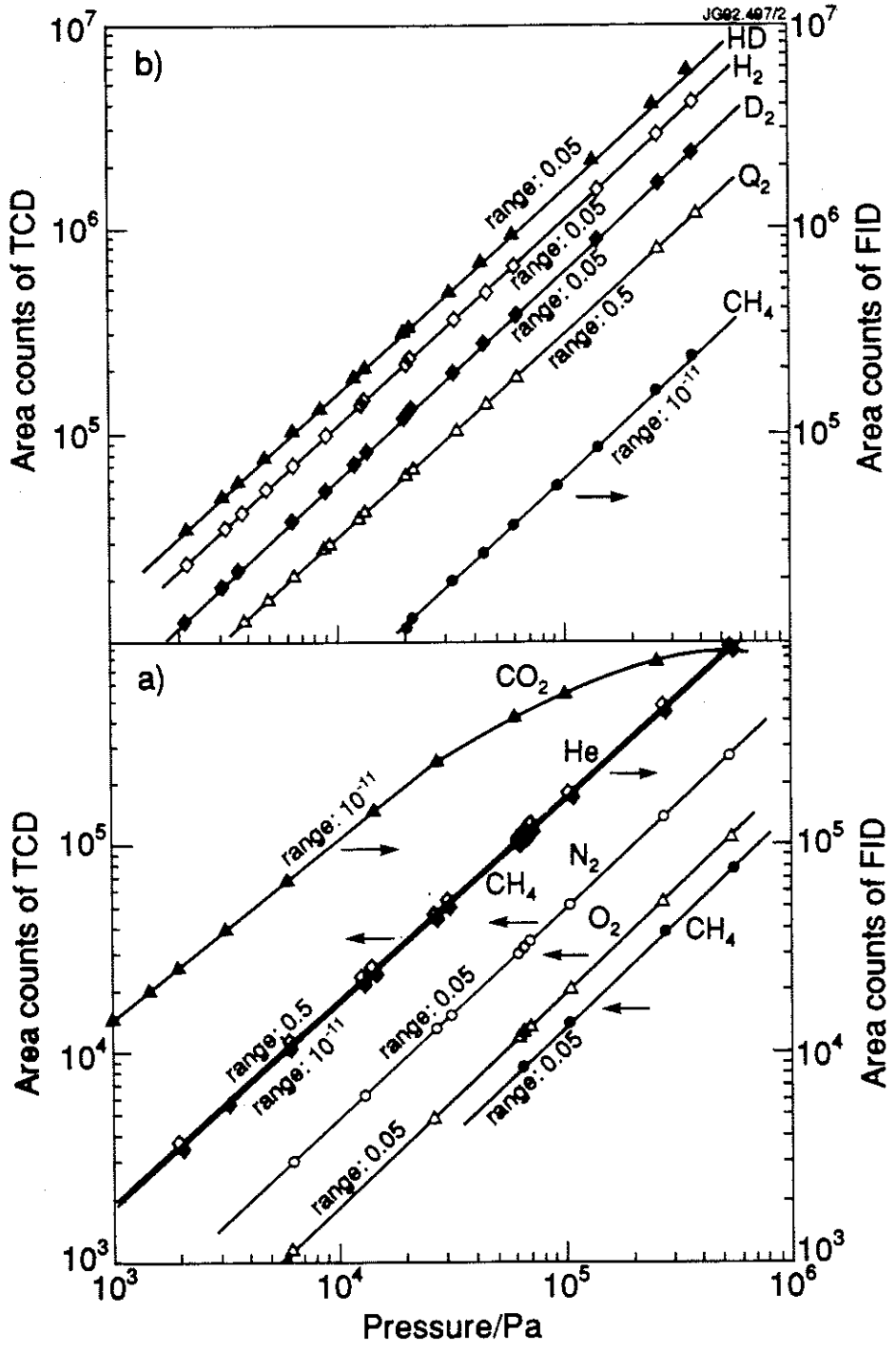

Fig. 3: Sensitivities of the GC-system as a function of pressure in the compression loop for gas mixtures 1 (lower part) and 2 (upper part), see Table 1.

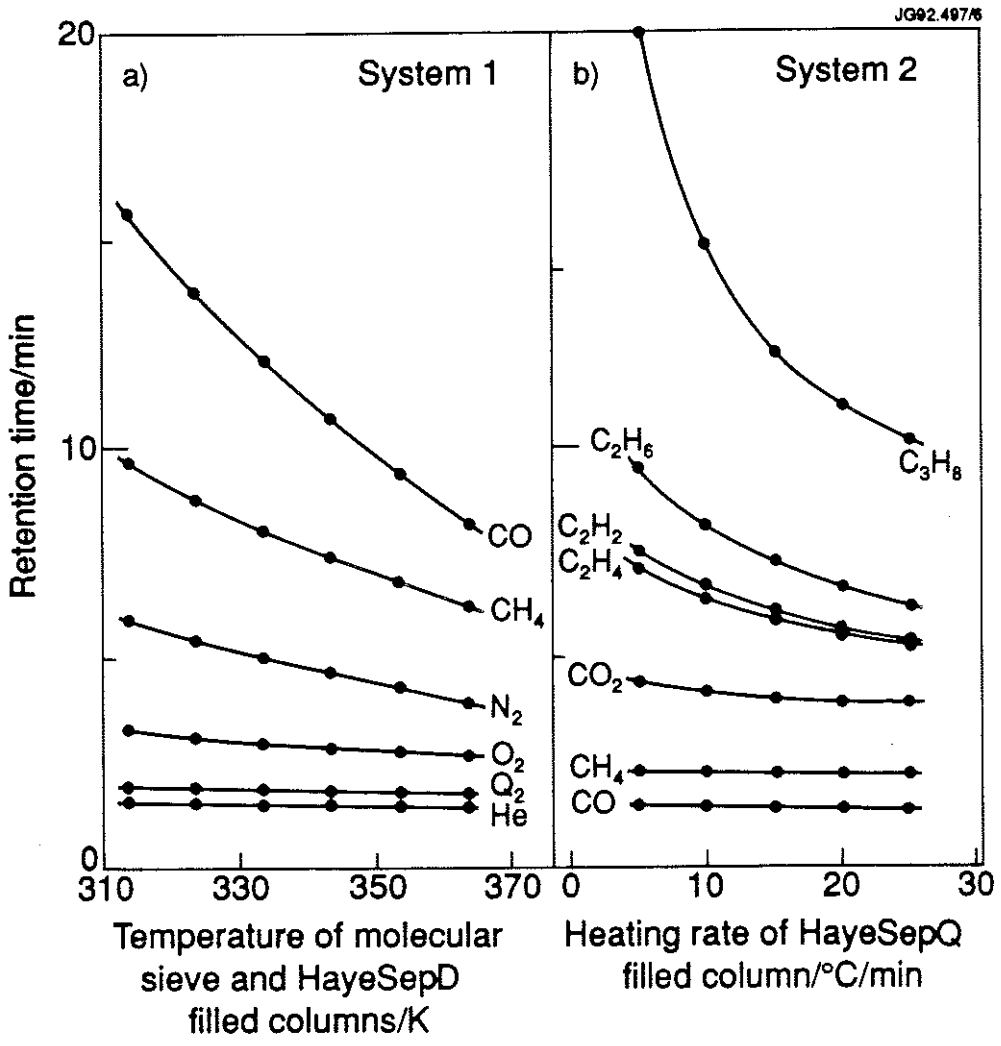

Fig. 4: Retention times as a function of column temperatures for system 1 (left hand side) and of column heating rates for system 2 (right hand side).

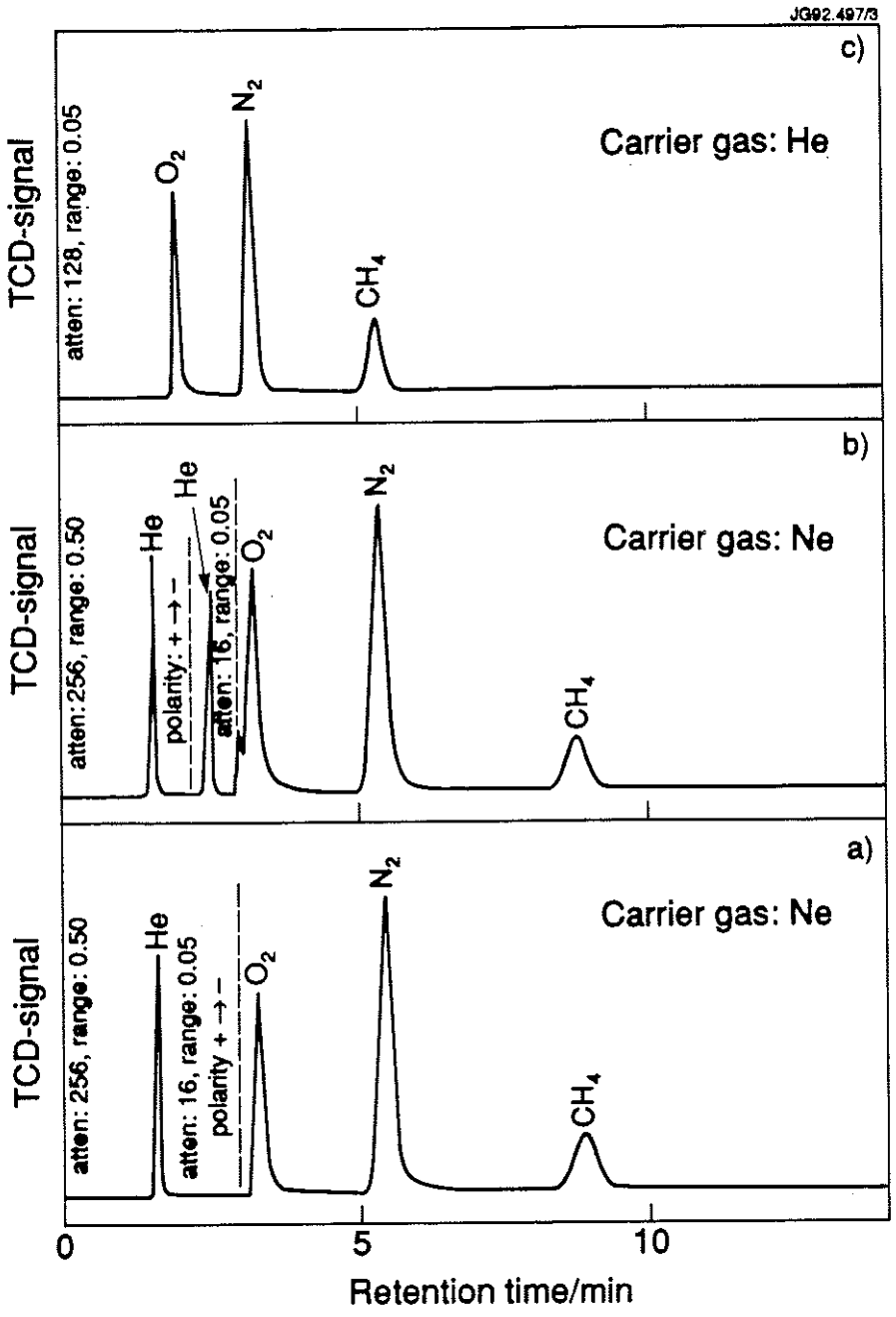

Fig. 5: TCD-chromatograms of gas mixture 1 (see table 1): for more details see text.

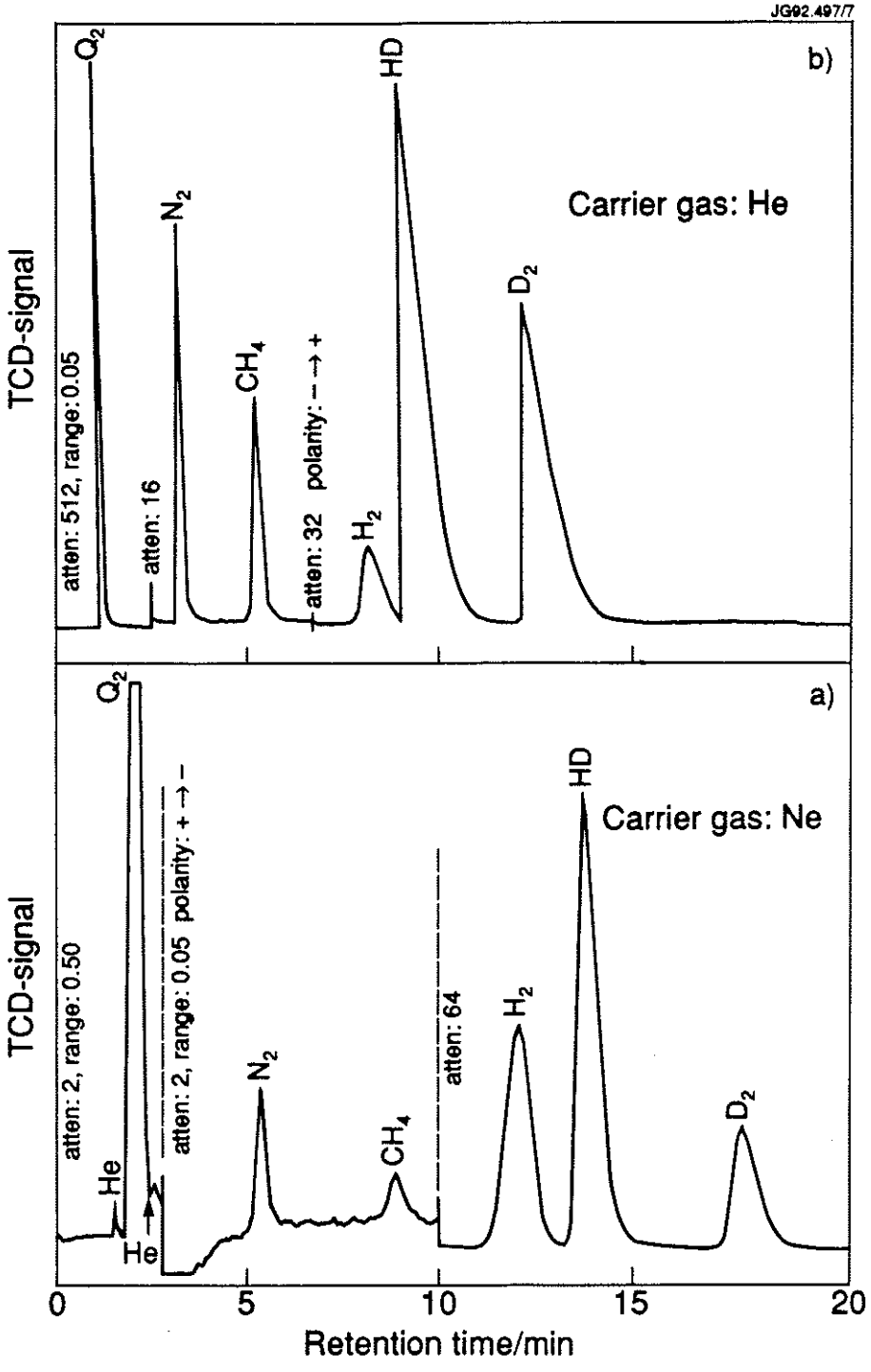

Fig. 6: TCD-chromatograms of gas mixture 2 (see table 1): for more details see text.

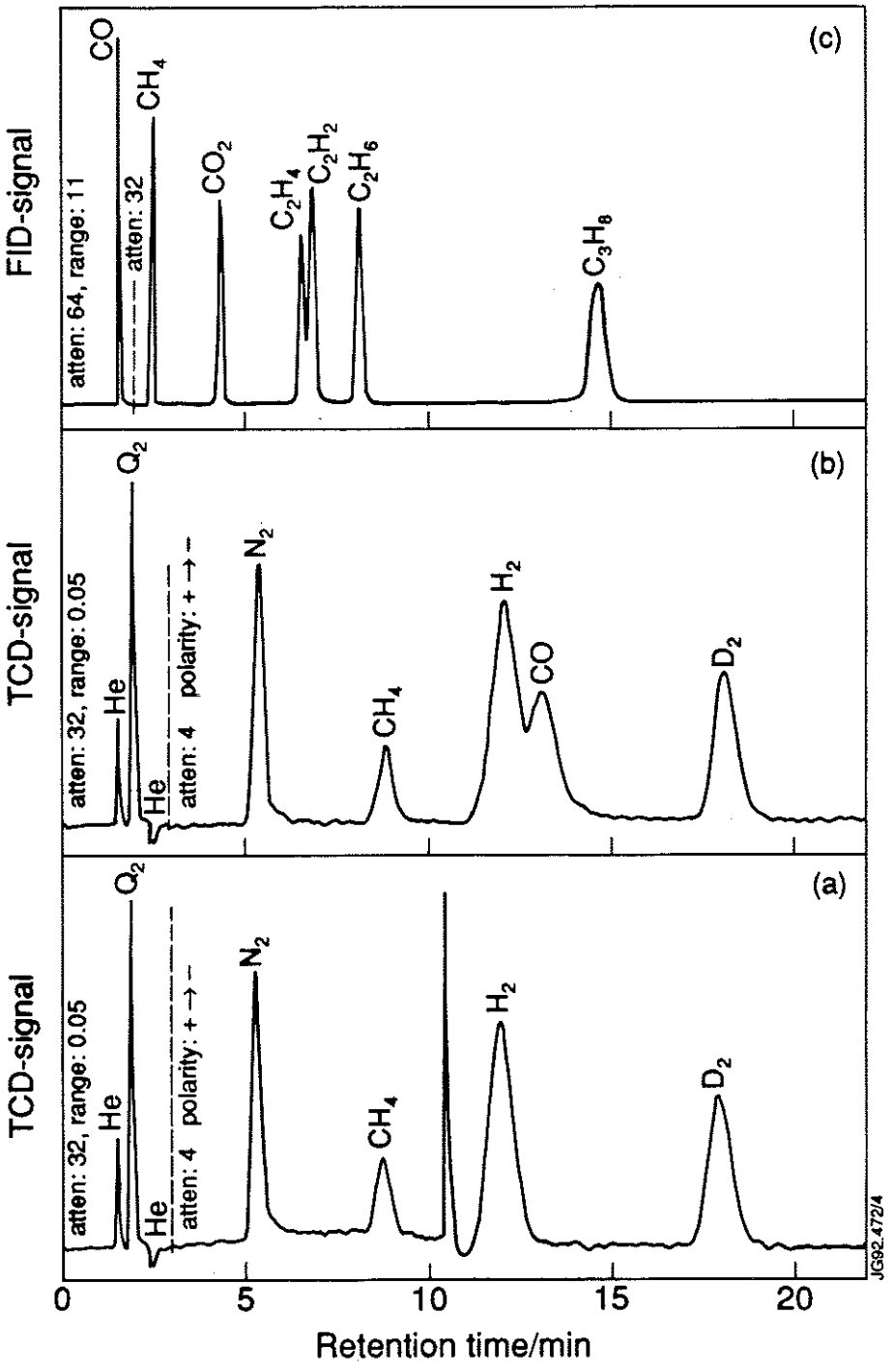

Fig. 7: TCD-chromatograms (a and b) and FID-chromatogram (c) of gas mixture 3 (see table 1): for more details see text.

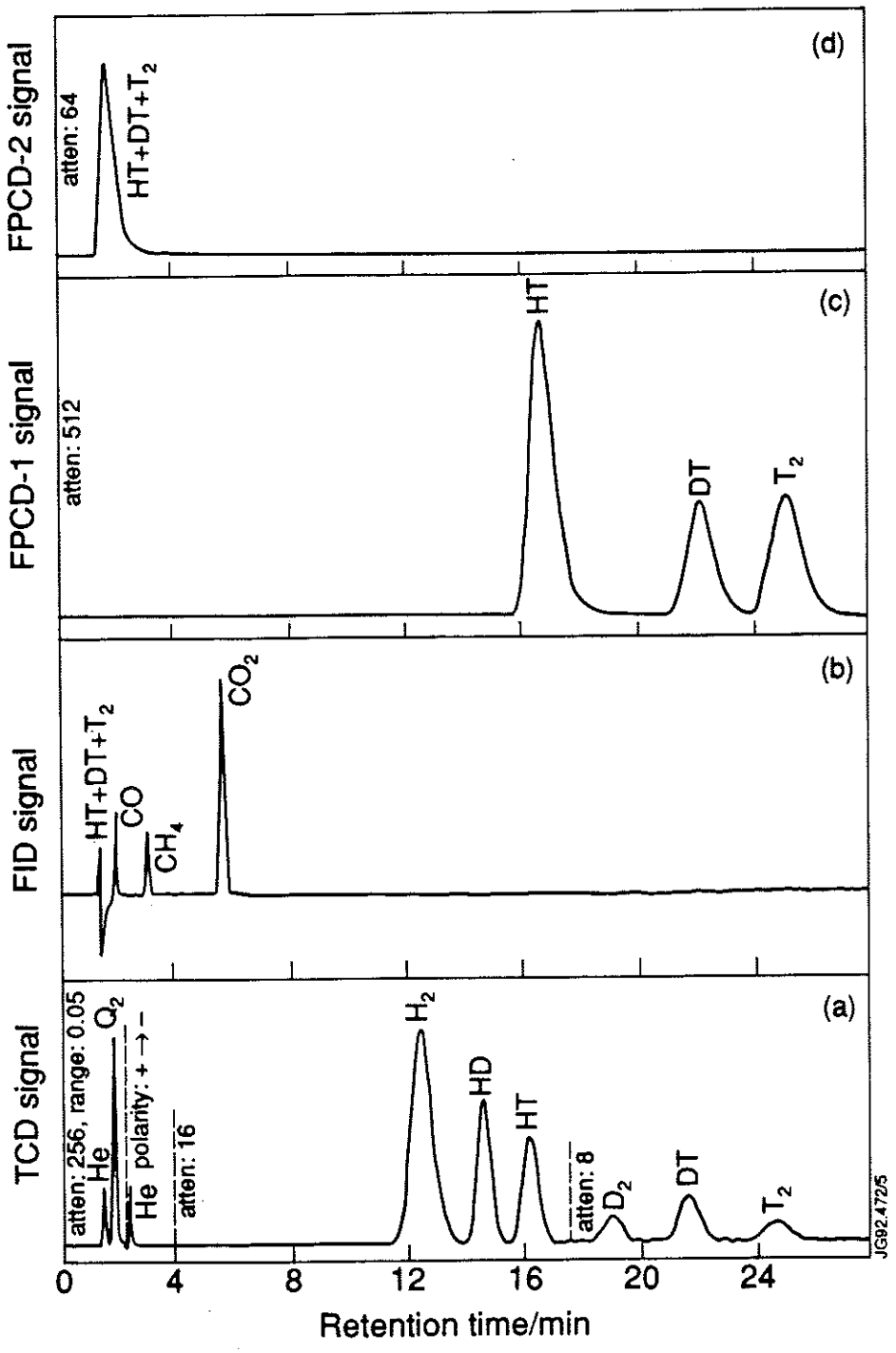

Fig. 8: TCD-chromatogram (a), FID-chromatogram (b) and FPCD-chromatograms (c and d) of gas mixture 4 (see table 1): for more details see text.

Appendix I

THE JET TEAM

JET Joint Undertaking, Abingdon, Oxon, OX14 3EA, U.K.

J.M. Adams[1], B. Alper, H. Altmann, A. Andersen[14], P. Andrew, S.Ali-Arshad, W. Bailey, B. Balet, P. Barabaschi, Y. Baranov, P. Barker, R. Barnsley[2], M. Baronian, D.V. Bartlett, A.C. Bell, G. Benali, P. Bertoldi, E. Bertolini, V. Bhatnagar, A.J. Bickley, D. Bond, T. Bonicelli, S.J. Booth, G. Bosia, M. Botman, D. Boucher, P. Boucquey, M. Brandon, P. Breger, H. Brelen, W.J. Brewerton, H. Brinkschulte, T. Brown, M. Brusati, T. Budd, M. Bures, P. Burton, T. Businaro, P. Butcher, H. Buttgereit, C. Caldwell-Nichols, D.J. Campbell, D. Campling, P. Card, G. Celentano, C.D. Challis, A.V.Chankin[23], A. Cherubini, D. Chiron, J. Christiansen, P. Chuilon, R. Claesen, S. Clement, E. Clipsham, J.P. Coad, I.H. Coffey[24], A. Colton, M. Comiskey[4], S. Conroy, M. Cooke, S. Cooper, J.G. Cordey, W. Core, G. Corrigan, S. Corti, A.E. Costley, G. Cottrell, M. Cox[7], P. Crawley, O. Da Costa, N. Davies, S.J. Davies[7], H. de Blank, H. de Esch, L. de Kock, E. Deksnis, N. Deliyanakus, G.B. Denne-Hinnov, G. Deschamps, W.J. Dickson[19], K.J. Dietz, A. Dines, S.L. Dmitrenko, M. Dmitrieva[25], J. Dobbing, N. Dolgetta, S.E. Dorling, P.G. Doyle, D.F. Düchs, H. Duquenoy, A. Edwards, J. Ehrenberg, A. Ekedahl, T. Elevant[11], S.K. Erents[7], L.G. Eriksson, H. Fajemirokun[12], H. Falter, J. Freiling[15], C. Froger, P. Froissard, K. Fullard, M. Gadeberg, A. Galetsas, L. Galbiati, D. Gambier, M. Garribba, P. Gaze, R. Giannella, A. Gibson, R.D. Gill, A. Girard, A. Gondhalekar, D. Goodall[7], C. Gormezano, N.A. Gottardi, C. Gowers, B.J. Green, R. Haange, A. Haigh, C.J. Hancock, P.J. Harbour, N.C. Hawkes[7], N.P. Hawkes[1], P. Haynes[7], J.L. Hemmerich, T. Hender[7], J. Hoekzema, L. Horton, J. How, P.J. Howarth[5], M. Huart, T.P. Hughes[4], M. Huguet, F. Hurd, K. Ida[18], B. Ingram, M. Irving, J. Jacquinot, H. Jaeckel, J.F. Jaeger, G. Janeschitz, Z. Jankowicz[22], O.N. Jarvis, F. Jensen, E.M. Jones, L.P.D.F. Jones, T.T.C. Jones, J-F. Junger, F. Junique, A. Kaye, B.E. Keen, M. Keilhacker, W. Kerner, N.J. Kidd, R. Konig, A. Konstantellos, P. Kupschus, R. Lässer, J.R. Last, B. Laundy, L. Lauro-Taroni, K. Lawson[7], M. Lennholm, J.Lingertat[13], R.N. Litunovski, A. Loarte, R. Lobel, P. Lomas, M. Loughlin, C. Lowry, A.C. Maas[15], B. Macklin, C.F. Maggi[16], G. Magyar, V. Marchese, F. Marcus, J. Mart, D. Martin, E. Martin, R. Martin-Solis[8], P. Massmann, G. Matthews, H. McBryan, G. McCracken[7], P. Meriguet, P. Miele, S.F. Mills, P. Millward, E. Minardi[16], R. Mohanti[17], P.L. Mondino, A. Montvai[3], P. Morgan, H. Morsi, G. Murphy, F. Nave[27], S. Neudatchin[23], G. Newbert, M. Newman, P. Nielsen, P. Noll, W. Obert, D. O'Brien, J. O'Rourke, R. Ostrom, M. Ottaviani, S. Papastergiou, D. Pasini, B. Patel, A. Peacock, N. Peacock[7], R.J.M. Pearce, D. Pearson[12], J.F. Peng[26], R. Pepe de Silva, G. Perinic, C. Perry, M.A. Pick, J. Plancoulaine, J-P. Poffé, R. Pohlchen, F. Porcelli, L. Porte[19], R. Prentice, S. Puppin, S. Putvinskii[23], G. Radford[9], T. Raimondi, M.C. Ramos de Andrade, M. Rapisarda[29], P-H. Rebut, R. Reichle, S. Richards, E. Righi, F. Rimini, A. Rolfe, R.T. Ross, L. Rossi, R. Russ, H.C. Sack, G. Sadler, G. Saibene, J.L. Salanave, G. Sanazzaro, A. Santagiustina, R. Sartori, C. Sborchia, P. Schild, M. Schmid, G. Schmidt[6], H. Schroepf, B. Schunke, S.M. Scott, A. Sibley, R. Simonini, A.C.C. Sips, P. Smeulders, R. Smith, M. Stamp, P. Stangeby[20], D.F. Start, C.A. Steed, D. Stork, P.E. Stott, P. Stubberfield, D. Summers, H. Summers[19], L. Svensson, J.A. Tagle[21], A. Tanga, A. Taroni, C. Terella, A. Tesini, P.R. Thomas, E. Thompson, K. Thomsen, P. Trevalion, B. Tubbing, F. Tibone, H. van der Beken, G. Vlases, M. von Hellermann, T. Wade, C. Walker, D. Ward, M.L. Watkins, M.J. Watson, S. Weber[10], J. Wesson, T.J. Wijnands, J. Wilks, D. Wilson, T. Winkel, R. Wolf, D. Wong, C. Woodward, M. Wykes, I.D. Young, L. Zannelli, A. Zolfaghari[28], G. Zullo, W. Zwingmann.

PERMANENT ADDRESSES

1. UKAEA, Harwell, Didcot, Oxon, UK.
2. University of Leicester, Leicester, UK.
3. Central Research Institute for Physics, Budapest, Hungary.
4. University of Essex, Colchester, UK.
5. University of Birmingham, Birmingham, UK.
6. Princeton Plasma Physics Laboratory, New Jersey, USA.
7. UKAEA Culham Laboratory, Abingdon, Oxon, UK.
8. Universidad Complutense de Madrid, Spain.
9. Institute of Mathematics, University of Oxford, UK.
10. Freien Universität, Berlin, F.R.G.
11. Royal Institute of Technology, Stockholm, Sweden.
12. Imperial College, University of London, UK.
13. Max Planck Institut für Plasmaphysik, Garching, FRG.
14. Risø National Laboratory, Denmark.
15. FOM Instituut voor Plasmafysica, Nieuwegein, The Netherlands.
16. Dipartimento di Fisica, University of Milan, Milano, Italy.
17. North Carolina State University, Raleigh, NC, USA
18. National Institute for Fusion Science, Nagoya, Japan.
19. University of Strathclyde, 107 Rottenrow, Glasgow, UK.
20. Institute for Aerospace Studies, University of Toronto, Ontario, Canada.
21. CIEMAT, Madrid, Spain.
22. Institute for Nuclear Studies, Otwock-Swierk, Poland.
23. Kurchatov Institute of Atomic Energy, Moscow, USSR
24. Queens University, Belfast, UK.
25. Keldysh Institute of Applied Mathematics, Moscow, USSR.
26. Institute of Plasma Physics, Academica Sinica, Hefei, P. R. China.
27. LNETI, Savacem, Portugal.
28. Plasma Fusion Center, M.I.T., Boston, USA.
29. ENEA, Frascati, Italy.

At 1st July, 1992